Journal of Applied Electrochemistry **31**: 165–173, 2001.

Regeneration of hexavalent chromium using a Bi-doped PbO_2 anode

K. MONDAL[1], N.V. MANDICH[2] and S.B. LALVANI[1]*
[1]*Department of Mechanical Engineering and Energy Processes, Southern Illinois University at Carbondale, Carbondale, IL 62901, USA*
[2]*HBM Electrochemical and Engineering Co., Lansing, IL, USA*
*(*author for correspondence, e-mail: lalvani@engr.siu.edu)*

Received 18 November 1999; accepted in revised form 22 August 2000

Key words: ceramic membrane, chromium, electromigration, electrooxidation, lead anode

Abstract

The rate of hexavalent chromium regeneration from trivalent chromium, present as an impurity in a chromium plating solution at the Bi-doped PbO_2 anode, is found to be approximately four times greater than the corresponding rate observed for a PbO_2 coated lead (anodized lead) anode. A mathematical model that takes into account species electromigration and associated mass transfer effects was developed and tested. Dynamic concentration data for various chromium species were used along with the mathematical model to evaluate the various rate parameters.

List of symbols

A area (m^2)
D diffusivity ($m^2\ h^{-1}$)
F faradaic constant (96 485 C $equiv^{-1}$)
k heterogeneous rate constant (m h^{-1})
k_m mass transfer rate constant (m h^{-1})
N constant of integration
n ionic charge (integer)
R universal gas constant (8.314 J $mol^{-1}\ K^{-1}$)
t time (s)
T temperature (K)
u ionic mobility ($m^2\ V^{-1}\ h^{-1}$)
V volume (m^3)
c_x anodic concentration (mol cm^{-3})
c_y cathodic concentration (mol cm^{-3})
z separation distance (cm)

Greek letters
v velocity (m h^{-1})
ϕ potential (V)

Subscripts
i ionic species
1 Cr^{3+}
2 $Cr_xO_y^{2-}$
a anode
c cathode
m mass transfer coefficient
p porous pot
01 oxidation of trivalent chromium
02 reduction to trivalent chromium
03 chromium deposition

1. Introduction

Hard chromium plating bath contains chromic acid solution, which is a mixture of dichromate, trichromate and tetrachromate anions. These anions are reduced to chromium metal in a multistep reduction sequence during cathodic electrodeposition [1]. However, simultaneous side reactions involve the incomplete reduction of polychromate anions to the trivalent cation of chromium as an impurity. Reverse etching of the metal substrate and dissolution of bus bars into the corrosive chromic acid leads to the build-up of contaminants. These impurities adversely affect the quality of metal deposition. Research is underway on developing technologies for the rejuvenation of heavily used or completely spent chromic acid. A number of such methods involve neutralization, electrodialysis, ion exchange and adsorption. However, these methods suffer from either the generation of large quantities of sludge, excessive use of chemicals (as in neutralization), nonselective metal removal (as in adsorption), poor membrane stability (as in electrodialysis), or high cost of operation [2, 3].

Mandich et al. [4] and Guddati et al. [5] demonstrated the use of a ceramic diaphragm for the removal metallic impurities in spent chrome plating baths. The cations (metallic impurities) in anode chamber (the compartment with the positively charged electrode) migrate to the cathode chamber (compartment containing the

negatively charged electrode) under the influence of an electric field. Sulfuric acid was used as the catholyte (solution in the cathode chamber) in their study. With the passage of time, the pH of the catholyte was observed to increase resulting in sludge formation. In a series of papers [6–9] we have demonstrated that spent chromic acid placed in the anode compartment can be purified under the application of an appropriate d.c. voltage which accomplishes electromigration of the metal cation impurities of iron, copper, trivalent chromium, nickel and zinc towards the negatively charged cathode compartment separated by a porous ceramic diaphragm. Polychromate anions stay in the anode chamber. As a result of the use of freshly prepared chromic acid as the catholyte, the pH in the cathode chamber does not increase significantly to cause metal hydroxide precipitation. In addition, electromigration of hexavalent chromium (as polychromate anion) to the anode compartment results in the return of chromium back in the plating solution.

Although PbO_2 present at the surface of a lead anode is known to oxidize (regenerates) trivalent chromium to its hexavalent form if sufficient electrode potential is applied, no data on the rate of reoxidation have been reported in open literature. In our previous work, a lead anode and cathode were used. The only effective way of reoxidation of Cr(III) to Cr(IV) involves the use of a high ratio (30:1) of anode to cathode area. This is not easy to achieve in plating practice, where 2–3:1 ratios are more practised and common. Therefore, an anode material that will increase the reoxidation rate will greatly benefit chromium platers. Reported research has shown that Bi-doped lead dioxide anodes are good candidates for oxidation of trivalent chromium [10]. In this paper, we present our findings on the rates of hexavalent chromium regeneration and describe the development of a mathematical model to validate the experimental data.

2. Model development

Two ionic species of chromium, that is, trivalent chromium (Cr^{3+}) and dichromate anion ($Cr_xO_y^{2-}$) are considered in this study. For the sake of simplicity, we consider that complete chromium reduction $Cr^{6+} \rightarrow Cr^0$ involves only dichromate ions and disregard higher polychromates. The movement of ith ionic species is assumed to be governed by its concentration gradient and electromigration according to the following flux equation [11]:

$$J_i = k_{mi}\Delta c_i - u_i c_i\left(\frac{\partial \phi}{\partial z}\right) \tag{1}$$

where the diffusion and convection terms are lumped together by an aggregate term that is characterized by the mass transfer coefficient, k_{mi}.

The following mathematical model includes mass balances on the two chromium species for each of the two compartments of the electrochemical cell. c_x and c_y represent the anode and cathode concentrations, respectively, and subscripts 1 and 2 represent Cr^{3+} and $Cr_xO_y^{2-}$, respectively. The model assumes that the diffusivity and mobility remain constant in accordance with the dilute solution theory. It is also hypothesized that the electrode potential at the anode and cathode remain constant over the course of an experiment and hence, the rate constants for the various electrochemical reactions listed below can be assumed to remain invariant:

$$Cr^{3+} \xrightarrow{k_{01}} Cr^{6+} \quad \left\lfloor \text{as } Cr_xO_y^{2-} \right\rfloor \quad \text{(anode)} \tag{2}$$

$$Cr^{6+} \xrightarrow{k_{02}} Cr^{3+} \quad \text{(cathode)} \tag{3a}$$

$$Cr^{6+} \xrightarrow{k_{03}} Cr^{0} \quad \text{(cathode)} \tag{3b}$$

2.1. Cr^{3+} balance

The schematic block diagram for the movement of trivalent chromium ions is presented in Figure 1. Trivalent chromium electromigrates from the anode chamber to the cathode chamber under the influence of an electric field. In addition, movement of ions between the two chambers also takes place under the influence of an

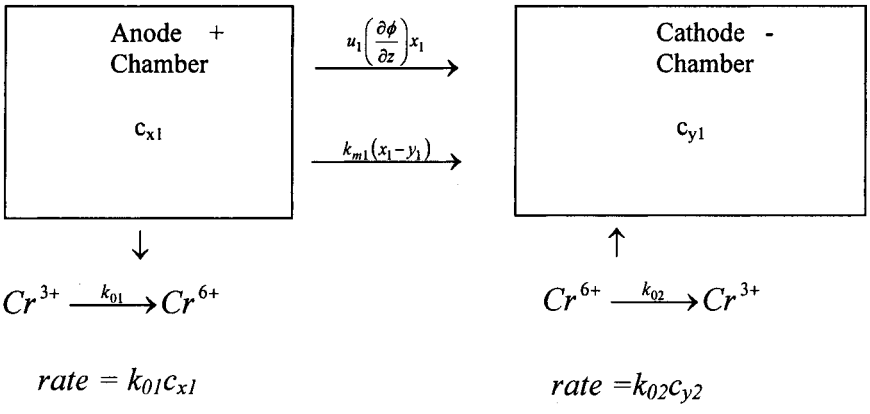

Fig. 1. Schematic for the mass balance of trivalent chromium.

existing concentration gradient. Due to reactions taking place at the electrode surfaces, further loss or generation of the trivalent chromium is observed in the cathode and anode compartments, respectively (as indicated by the arrows at the bottom of Figure 1). The mass balance of each species in each chamber is described by the following equation:

$$\text{Accumulation} = \text{In} - \text{Out} + \text{Reaction} \tag{4}$$

Anode: The mass balance for trivalent chromium ions in the anodic chamber can be written as

$$V_a \frac{dc_{x1}}{dt} = [0] - \left[u_1\left(\frac{\partial\phi}{\partial z}\right)c_{x1}A_p + k_{m1}(c_{x1} - c_{y1})A_p\right] - [k_{01}c_{x1}A_a] \tag{4a}$$

The above expression can be rewritten in the form:

$$\frac{dc_{x1}}{dt} = -a_1c_{x1} + b_1c_{y1} \tag{5}$$

The coefficients in Equation 5 are listed in Table 1.

Cathode: For the cathode chamber, the mass balance expression for trivalent chromium is given by:

$$V_c \frac{dc_{y1}}{dt} = \left[u_1\left(\frac{\partial\phi}{\partial z}\right)c_{x1}A_p + k_{m1}(c_{x1} - c_{y1})A_p\right] - [0] + [k_{02}c_{y2}A_c] \tag{4b}$$

which can be rewritten as

$$\frac{dc_{y1}}{dt} = a_1^1c_{x1} - b_1^1c_{y1} + h_1^1c_{y2} \tag{6}$$

The coefficients in Equation 6 are listed in Table 1.

2.2. $Cr_xO_y^{2-}$ balance

Figure 2 shows the fate of the $Cr_xO_y^{2-}$ anion during the process. In addition to the movement of hexavalent chromium under a potential and concentration gradient, trivalent chromium is oxidized to the chromate anion at the anode (as shown by the arrow below the box) while the hexavalent chromium species are reduced to trivalent chromium or chromium metal at the cathode (as shown by the arrows on the right and below the box). For the hexavalent chromium species, the differential mass balances on the chromium anion for the anode and cathode compartments are given by the following equations:

Table 1. Coefficients in Equations 5–8

$a_1 = k_{01}\sigma_3 + \left[k_{m1} + u_1\left(\frac{\partial\phi}{\partial z}\right)\right]\sigma_1$
$b_1 = k_{m1}\sigma_1$
$a_1^1 = \left[k_{m1} + u_1\left(\frac{\partial\phi}{\partial z}\right)\right]\sigma_2$
$b_1^1 = b_1\left(\frac{\sigma_2}{\sigma_1}\right)$
$h_1^1 = k_{02}\sigma_4$
$a_2 = k_{01}\sigma_3$
$b_2 = k_{m2}\sigma_1$
$h_2 = \left[k_{m2} + u_2\left(\frac{\partial\phi}{\partial z}\right)\right]\sigma_1$
$a_2^1 = b_2\left(\frac{\sigma_2}{\sigma_1}\right)$
$b_2^1 = (k_{02} + k_{03})\sigma_4 + u_2\left(\frac{\partial\phi}{\partial z}\right)\sigma_2 + k_{m2}\sigma_2$
$\sigma_1 = A_p/V_a$
$\sigma_2 = A_p/V_c$
$\sigma_3 = A_a/V_a$
$\sigma_4 = A_c/V_c$

$$\frac{dc_{x2}}{dt} = a_2c_{x1} - b_2c_{x2} + h_2c_{y2} \tag{7}$$

$$\frac{dc_{y2}}{dt} = a_2^1c_{x2} - b_2^1c_{y2} \tag{8}$$

Coefficients in Equations 5–8 are listed in Table 1. The four coupled equations (Equations 5–8) are solved by an elimination of variables method outlined in Appendix 1.

3. Experimental details

3.1. *Chemicals*

The lead electrodes were made by cutting 3/32 inch thick sheets obtained by McMaster Carr (Chicago, IL) into 10 cm × 1 cm pieces. All other chemicals were obtained from Alfa Aesar (Ward Hill, MA).

3.2. *Preparation of anodes*

In accordance to the experimental conditions described by Vora et al. [12], a passivating film was formed on the

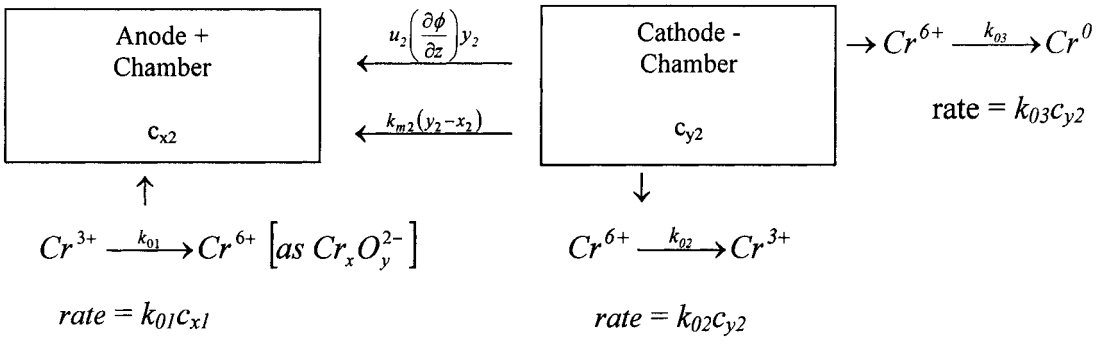

Fig. 2. Schematic for the mass balance of hexavalent chromium.

Pb surface by immersing it in a 3 M H_2SO_4 solution for 3 h at 0.4 V vs SCE. The potential of this electrode was then spiked momentarily to 2.3 V vs SCE to allow for the creation of nucleating sites for PbO_2 in the passive film. Finally, the electrode was anodized at a constant potential of 1.7 V vs SCE for a period of 8 h. The Bi-doped PbO_2 layer was deposited on the PbO_2 coated lead from a bath containing 0.4 mM $Bi(NO_3)_2$, 0.12 M $Cu(NO_3)_2$, 10 mM $Pb(NO_3)_2$ along with 0.1 g L^{-1} of sodium dodecyl sulfate (SDS) in 1 M perchloric acid.

3.3. *Preparation of solutions*

A typical spent chromic acid bath (anolyte) contains Cr(III)/Cr(VI) in the ratio of 1:25. However, for the purpose of this investigation four different ratios of Cr(III)/Cr(VI) were prepared from chromium sulfate and chromium trioxide while the sulfate concentration was maintained at 2.5 g L^{-1}. The total chromium concentration of the synthetic spent solutions was kept at 130 g L^{-1}, which corresponds to a concentration of 250 g L^{-1} of CrO_3 used in hard chromium plating baths. The composition of the catholyte used in this study was identical to that of the anolyte in order to avoid the occurrence of any concentration gradient across the ceramic membrane prior to the application of an electric field.

3.4. *Regeneration*

The electrochemical oxidation of Cr(III) was conducted in a divided electrolytic cell as shown in Figure 3. The design parameters of the electrochemical cell are provided in Table 2.

Table 2. Physical specifications of the reactor

A_p/m^2	5.07×10^{-4}
A_a/m^2	16×10^{-4}
A_c/m^2	17.59×10^{-4}
V_a/m^3	0.35×10^{-3}
V_c/m^3	0.15×10^{-3}
σ_1/m^{-1}	1.45
σ_2/m^{-1}	3.38
σ_3/m^{-1}	4.57
σ_4/m^{-1}	11.73

3.5. *Analysis*

The analysis of the solutions at different times in both the cathode and the anode chamber were analysed for Cr(VI) content with an ion chromatograph (Dionex Corporation, Sunnyvale (CA), model DX 500) and a 4 mm CS5A column. The chromatograph was equipped with a conductivity cell (CD 20). The total chromium was measured using a Buck Scientific 210 VGP atomic absorption spectrophotometer at a wavelength of 357.9 nm.

4. Results and discussion

Figures 4–7 show hexavalent chromium and trivalent chromium concentration against time data from four experiments. The initial hexavalent chromium concentration in these four experiments was 29, 98, 108 and 127 g L^{-1}, respectively. The total chromium concentration in all the experiments (except for the experiment in which an initial hexavalent chromium concentration of 29 g L^{-1} was used) was maintained at 130 g L^{-1}

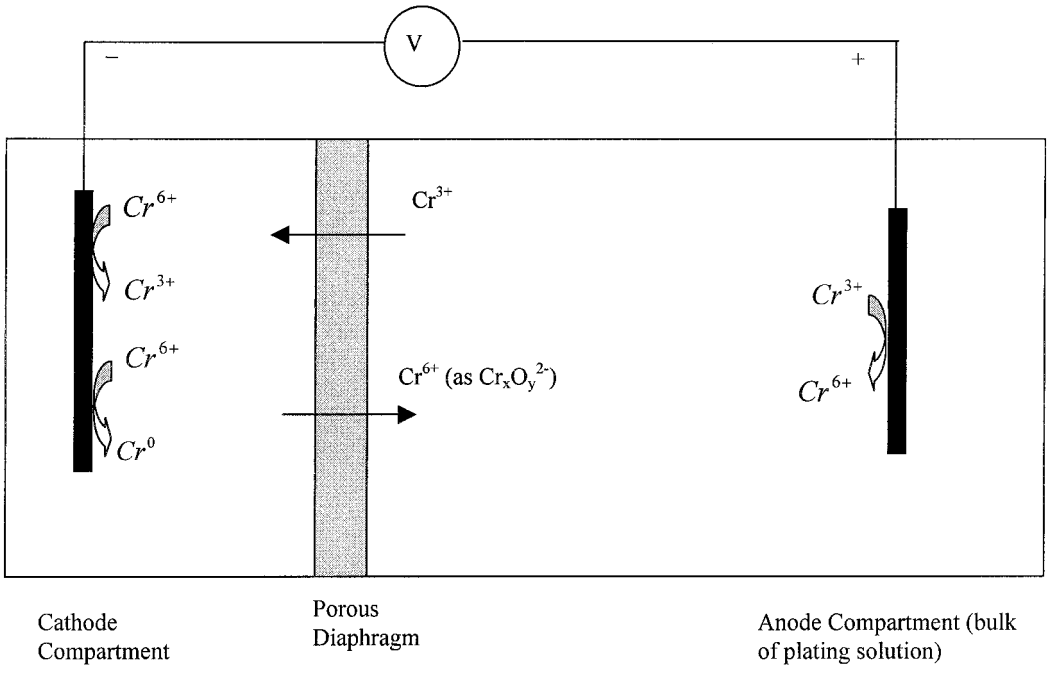

Fig. 3. Schematic of the experimental set-up.

(corresponding to 250 g L^{-1} of CrO_3). Bi-doped lead dioxide on a PbO_2 coated lead substrate was used as anode for these experiments. A more dilute solution (43 g L^{-1} of total chromium) was used for the experiment that used an initial hexavalent chromium concentration of 29 g L^{-1}. Both Bi-doped lead dioxide on PbO_2 coated lead and anodized lead were used as anodes for experiments conducted at this concentration. 2.5 g L^{-1} of sulfate, which acts as a catalyst for chromium deposition, was added to the chromium solution. A constant voltage of 5 V was applied across the electrochemical cell. The experiments were carried out at a constant temperature of 45 °C. When a low initial concentration of chromium was used, the concentration of regenerated hexavalent chromium increased rather rapidly in the anode compartment. For example, the hexavalent chromium concentration increased by about 218% in about 23 h (Figure 4) when the initial hexavalent chromium concentration in the solution was 29 g L^{-1}. The trivalent chromium concentration decreases with time and reduces to a negligible amount at the end of the experiment. As expected, the hexavalent chromium concentration in the cathode compartment decreases with time due to its migration to the anode as well as by its reduction to trivalent chromium and metallic chromium at the cathode.

When an initial chromium (Cr^{6+}) concentration of 98 g L^{-1} was used (Figure 5), its concentration initially increases with time in the anode compartment, reaches a maximum of about 120 g L^{-1} and then declines somewhat with further increase in time. The initial increase in concentration is attributable to electromigration of hexavalent chromium from the cathode to the anode as well as electrocatalytic anodic oxidation of trivalent

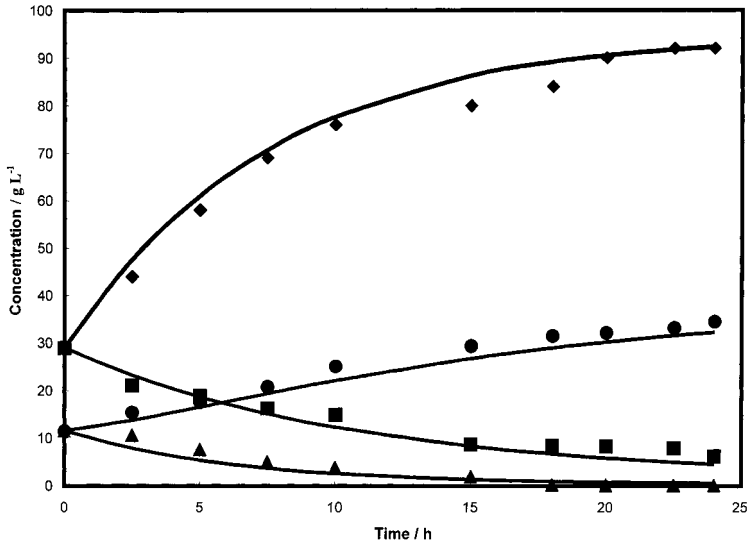

Fig. 4. Concentration against time for chromium species in both compartments. Initial concentration of hexavalent chromium of 29 g L^{-1}. Bi-doped lead dioxide anode was used. Key: (◆) Cr^{6+} (anode); (■) Cr^{6+} (cathode); (▲) Cr^{3+} (anode); (●) Cr^{3+} (cathode).

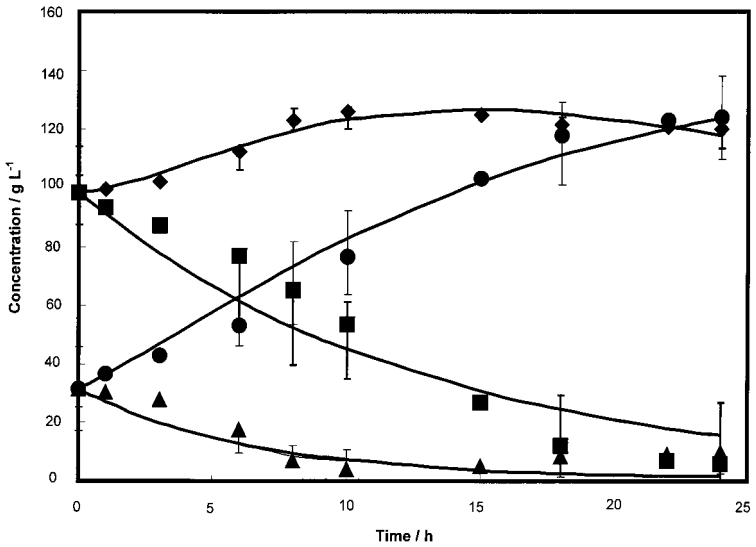

Fig. 5. Concentration against time for chromium species in both compartments. Initial concentration of hexavalent chromium of 98.5 g L^{-1}. Bi-doped lead dioxide anode was used. Key: as given in Figure 4.

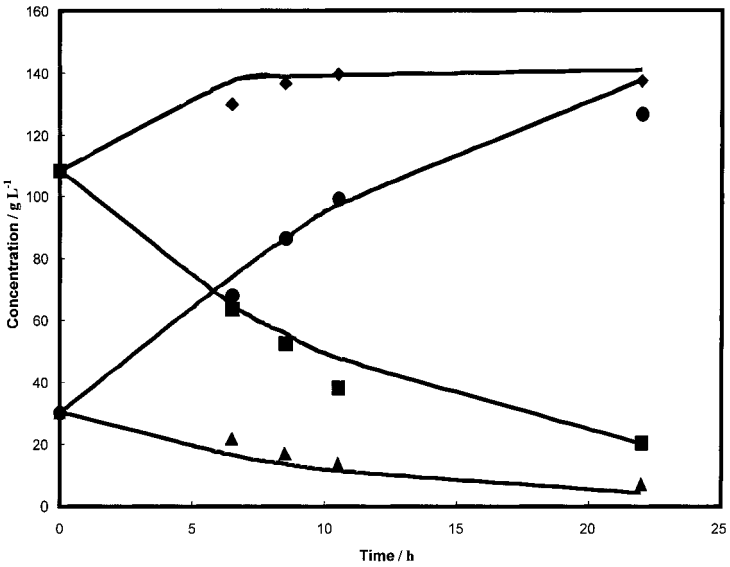

Fig. 6. Concentration against time for chromium species in both compartments. Initial concentration of hexavalent chromium of 108 g L^{-1}. Bi-doped lead dioxide anode was used. Key: as given in Figure 4.

chromium to hexavalent chromium. However, when the hexavalent chromium concentration in the anode compartment is significantly greater than that in the cathode compartment, mass transfer rate of the hexavalent chromium from the anode to the cathode compartment (back diffusion) becomes significant in comparison to its rate of electromigration from the cathode to the anode. In addition, the rate of hexavalent chromium regeneration decreases with time due to a decrease in the trivalent chromium concentration in the anode compartment. This experiment was repeated twice and the standard error bars from the mean are shown in Figure 5. The increase in hexavalent chromium concentration for relatively large initial concentrations of hexavalent chromium (Figures 5, 6 and 7) was relatively modest. Nonetheless, a maximum hexavalent chromium concentration of 130–135 g L^{-1} in the anode compartment was achievable when the initial concentration of total chromium was approximately 130 g L^{-1}. At concentrations greater than 130 g L^{-1}, the mass transfer of hexavalent chromium predominates over the processes of electromigration and oxidation of trivalent chromium.

To compare the effect of various anode materials on the increase in hexavalent chromium concentration, one experiment using lead dioxide as anode (at the lowest initial Cr^{6+} concentration of 29 g L^{-1}) was carried out. The data in Figure 8 show that Bi-doped PbO_2 is more effective than PbO_2. Whereas the use of a PbO_2 coated lead anode results in only a 67% increase in the

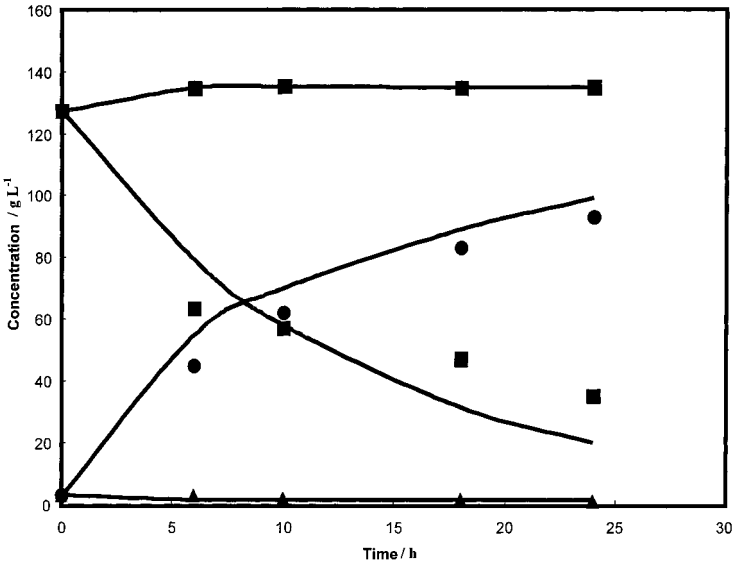

Fig. 7. Concentration against time for chromium species in both compartments. Initial concentration of hexavalent chromium of 127 g L^{-1}. Bi-doped lead dioxide anode was used. Key: as given in Figure 4.

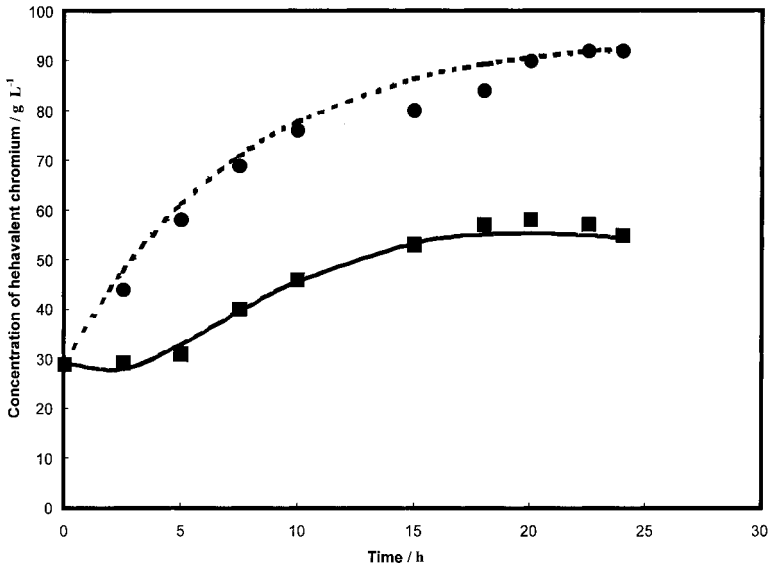

Fig. 8. Concentration against time for chromium species in both compartments. Initial concentration of hexavalent chromium of 29 g L^{-1}. Lead dioxide anode was used. Key: (■—■) lead dioxide; (● - - - ●) Bi-doped lead dioxide.

hexavalent chromium concentration, the Bi-doped PbO_2 results in about 218% increase in hexavalent chromium concentration under identical experimental conditions.

The experimental data shown in Figures 4–7 were fitted to the mathematical model developed in this paper (Appendix 1). The constants (Table 1) described in the model are a combination of various physical properties, design variables and operating parameter. In addition, the constants a_1, c_1 and a_2 are a function of some of the other constants in Table 1. The independent constants (b_1, a_1^1, h_1^1, a_2, b_2, h_2, b_2^1) described in the model and the exponents (m_1, m_2, m_3, m_4) were estimated using the Levenberg–Marquadt algorithm for non-linear parameter estimation [13]. The objective function was to minimize the total errors between experimental and predicted values for each species after normalization with the measurement error under the constraint that the errors for individual species were also minimized. The values of constants of integration, N_i's, were determined analytically by solving for the initial conditions, based on the estimated values of the constants and exponents. The solid lines in Figures 4–7 represent the predicted concentration profiles based on the estimated constants. A good agreement between the experimental and predicted values is observed in these Figures.

Table 3 lists the mean values of the physical parameters calculated from the estimated values of the fitted constants used in the development of the model while Tables 4 and 5 list the fitted exponents (m_i's) and the corresponding N_i's. The results (Table 3) correspond closely to that found in literature [14]. For example, the mobility of trivalent chromium was found to be 30.2×10^{-5} m^2 V^{-1} h^{-1}, while that reported in literature is 20.5×10^{-5} m^2 V^{-1} h^{-1}. The values of mass transfer coefficients and reaction rate constants are of the same order of magnitude (10^{-5} and 10^{-2} m h^{-1}, respectively) as those reported in our previous findings [9]. The estimated values of the mass transfer coefficients show that the complex chromate anions have a greater mobility as compared to that of the trivalent chromium cation. The estimated values of the exponents (m_i's)

Table 3. Estimated physical constants

	Bi-doped PbO_2 anode	PbO_2 anode
k_{m1}/m h^{-1}	27.1×10^{-5}	27.1×10^{-5}
k_{m2}/m h^{-1}	90.2×10^{-5}	90.2×10^{-5}
k_{01}/m h^{-1}	66.8×10^{-3}	15.8×10^{-3}
k_{02}/m h^{-1}	13.8×10^{-3}	13.8×10^{-3}
u_1/m^2 V^{-1} h^{-1}	30.2×10^{-5}	30.2×10^{-5}
u_2/m^2 V^{-1} h^{-1}	80.9×10^{-5}	80.9×10^{-5}
k_{03}/m h^{-1}	1.8×10^{-3}	1.8×10^{-3}

Table 4. Estimated values for the exponents in Equations A8, A10, A11 and A12

Initial Cr^{6+}	Bi-doped PbO_2 anode				PbO_2 anode
	29 g L^{-1}	98.5 g L^{-1}	108 g L^{-1}	127 g L^{-1}	29 g L^{-1}
m_1	-2×10^{-5}	−0.0050	−0.0031	−0.0076	−0.0032
m_2	−0.0865	−0.0759	−0.0823	−0.0745	−0.0865
m_3	−0.1401	−0.1374	−0.1412	−0.1250	−0.0990
m_4	−0.1510	−0.1505	−0.1496	−0.1409	−0.1839

Table 5. Estimated values for the coefficients in Equations A8, A10, A11 and A12

Initial Cr^{6+}	Bi-doped PbO_2 anode				PbO_2 anode
	29 g L^{-1}	98.5 g L^{-1}	108 g L^{-1}	127 g L^{-1}	29 g L^{-1}
c_1	0.3487	1.5378	0.9898	2.7534	−0.6987
c_2	−1.1487	−3.4420	−2.4123	−6.0283	9.6771
c_3	−0.2921	−3.9532	−6.0804	1.7976	2.9894
c_4	12.5921	37.3673	37.8029	4.5771	−0.4678

satisfy the condition of being the roots of Equation A9 in Appendix 1. Since all exponents are negative, the rates of change in concentration decreases with time and may eventually change the direction of change. This is reflected in the fact that the concentration of hexavalent chromium in the anode chamber decreases while that in the cathode chamber increases after around 20 hours of running the experiments. The values of the exponents are found to vary with concentration, since the value of m_i is dependent on concentration-dependent terms such as diffusivity, mobility and mass transfer rate constant [15]. The anodic and cathodic potentials were monitored as a function of time. The potentials were essentially invariant in time, as was assumed in the model.

As seen from the values of k_{01} (Table 3), the rate of oxidation of trivalent chromium to hexavalent chromium is found to be over four times greater in the case of the Bi-doped anode than that of the simple commercial PbO_2 coated lead electrode for the same applied voltage and the same initial concentrations. This result is reflected in the high concentration of hexavalent chromium in the anode chamber (Figure 8). The rate of oxidation of trivalent chromium at the lead dioxide anode is low because the electrode has a high overpotential for oxygen evolution. Although, on the one hand, lead dioxide anodes are used in chromium plating solution to avoid oxygen evolution as it would lead to lower efficiencies for deposition. The lack of oxygen results in a relatively poor oxidation rate. On the other hand, addition of bismuth sites on the lead dioxide anode, results in enhanced adsorption of hydroxyl ions from water. These hydroxyl ions are transferred to the lead sites for the oxygen transfer to take place according to the mechanism proposed by Hsiao and Johnson [16]. The rapid transfer of oxygen leads to a higher oxidation rate of trivalent chromium at the doped electrode.

Thus, an ideal anode for enhanced oxygen-transfer reactivity can be envisioned as an inert matrix having a large oxygen evolution overpotential into which is incorporated a low-density array of catalytic sites characterized by low O_2 evolution overpotential. Owing to the low area of the sites, the background current for oxygen evolution would be minimal. However, a high flux of the diffusing trivalent chromium will be oxidized to hexavalent chromium at these sites. If the inter-site distances were less than the diffusion layer thickness, highly efficient oxygen transfer reactions can be expected at the electrode.

5. Conclusions

Hard chrome plating solution was rejuvenated by oxidation of trivalent chromium in a porous pot using lead dioxide and bismuth doped lead dioxide anodes. The regeneration of hexavalent chromium was conducted at four different concentrations of trivalent chromium and two different concentrations of total chromium. The Bi-doped lead dioxide anode results in faster oxidation kinetics of trivalent chromium. A model was developed for the regeneration process and validated against experimental data. The model was used to estimate the physical parameters such as the mass transfer coefficient, rate constants of the various reactions and the mobility of the trivalent and hexavalent chromium ions. The estimated values obtained from regression were in good agreement with those reported in the literature.

Acknowledgements

Financial support for this research was provided by Illinois Waste Management and Research, Champaign, Illinois and the Materials Technology Center, Southern Illinois University, Carbondale, IL.

References

1. N.V. Mandich, *Plat. Surf. Finish.* **84** (6) (1997) 67.
2. N.V. Mandich, 'Removal of Metallic Impurities from Plating Solutions by Electrocoagulation', *AESF Chromium Colloquium*, Vol. 36 (AESF, Orlando, FL, Jan. 1994).
3. S.B. Lalvani and N.V. Mandich, 'Removal of Metallic Impurities in Chromium Plating Solutions by Electrocoagulation', Illinois Waste Management and Research Center, Champaign, IL, Project 97025 (1997).
4. N.V. Mandich, C-C. Lee and J.R. Selman, *Plat. Surf. Finish.* **84** (12) (1997) 82.
5. S.L. Guddati, T.M. Holsen, C-C. Li, J.R. Selman and N.V. Mandich, *J. Appl. Electrochem.* **29** (1999) 1129.
6. S.B. Lalvani and N.V. Mandich, 'Removal of Metallic Impurities in Chromium Plating Solutions by Electrocoagulation-Phase I', Project No. 97025, Final Report to Illinois Waste Management and Research Center, Champaign, IL (1998).
7. J. Pattanayak, K. Mondal, N.V. Mandich, T. Wiltowski and S.B. Lalvani, *Metal Finish.* **98** (3) (2000) 39.
8. J. Pattanayak, N.V. Mandich, K. Mondal, T. Wiltowski and S.B. Lalvani, *Environmental Technol.* **20** (1999) 317.
9. S.B. Lalvani, K. Mondal, J. Pattanayak, N.V. Mandich and T. Wiltowski, *J. Electrochem. Soc.*, under review.
10. K.L. Pamplin and D.C. Johnson, *J. Electrochem. Soc.* **143** (1996) 2119.
11. A.J. Bard and L.R. Faulkner, 'Electrochemical Methods – Fundamentals and Applications' (J. Wiley & Sons, New York, 1980).
12. R.J. Vora, S.R. Taylor and G.E. Stoner, *in* F. Hine et al., 'Factors Affecting the Performance of PbO_2 Anodes in the Generation of Hexavalent Chromium' Proceedings of the Symposium on Performance of Electrodes for Industrial and Chemical Processes (The Electrochemical Society, 1989), p. 279.
13. D.A. Ratkowsky, 'Nonlinear Regression Modeling: A Unified Practical Approach' (Marcel Dekker, New York, 1983).
14. S.L. Guddati, T.M. Holsen and J.R. Selman, 'Optimization of Porous Ceramic Diaphragm Cell Operation for the Removal of Metallic Impurities from Chrome Plating Bath', *Report for Summer Research Grant Program* (AESF, Orlando, FL, 1995).
15. R.E. Treybal, 'Mass Transfer Operations', 3rd edn (McGraw-Hill, London, 1980), pp 35–37.
16. Y-L. Hsiao and D.C. Johnson, *J. Electrochem. Soc.* **136** (1989) 3704.

Appendix 1

Consider the following coupled differential equations:

$$\frac{dc_{x1}}{dt} = -a_1 c_{x1} + b_1 c_{y1} \tag{A1}$$

$$\frac{dc_{y1}}{dt} = a_1^1 c_{x1} - b_1^1 c_{y1} + h_1^1 c_{y2} \tag{A2}$$

$$\frac{dc_{x2}}{dt} = a_2 c_{x1} - b_2 c_{x2} + h_2 c_{y2} \tag{A3}$$

$$\frac{dc_{y2}}{dt} = a_2^1 c_{x2} - b_2^1 c_{y2} \tag{A4}$$

From Equation A1:

$$c_{y1} = \frac{1}{b_1}\left[\frac{dc_{x1}}{dt} + a_1 c_{x1}\right] \tag{A1a}$$

Substitution of Equation A1a into Equation A2 and solving for y_2 gives

$$c_{y2} = \frac{1}{b_1 h_1^1}\left[\frac{d^2 c_{x1}}{dt^2} + q\frac{dc_{x1}}{dt} - r c_{x1}\right] \tag{A5}$$

where (i) $q = a_1 + b_1^1$ and (ii) $r = a_1^1 b_1 - a_1 b_1^1$.

Substitution of Equation A5 into Equation A4 and solving for x_2 gives

$$c_{x2} = \frac{1}{a_2^1 b_1 h_1^1}\left[\frac{d^3 c_{x1}}{dt^2} + p\frac{d^2 c_{x1}}{dt^2} - f\frac{dc_{x1}}{dt} - g\, c_{x1}\right] \tag{A6}$$

where (iii) $p = q + b_2^1$, (iv) $f = r - q\, b_2^1$ and (v) $g = r\, b_2^1$.

Substitution of Equations A5 and A6 into Equation A3 and solving for c_{x1} gives

$$\frac{d^4 c_{x1}}{dt^4} + (b_2 + p)\frac{d^3 c_{x1}}{dt^3} + (b_2 p - a_2^1 h_2 - f) \times \frac{d^2 c_{x1}}{dt^2} - (g + b_2 f + a_2^1 h_2 q)\frac{dc_{x1}}{dt} - (b_2 g - a_2^1 h_2 r + a_2 a_2^1 b_1 h_1^1) x_1 = 0 \tag{A7}$$

Solution to the above fourth order differential equation is given by

$$c_{x1} = \sum_{j=1}^{4} N_j e^{m_j t} \tag{A8}$$

where N_j is the constant of integration and the four exponents, m_j are given by the roots of the following algebraic expression:

$$D^4 + (b_2 + p)D^3 + (b_2 p - a_2^1 h_2 - f)D^2 - (g + b_2 f + a_2^1 h_2 q)D - (b_2 g - a_2^1 h_2 r + a_2 a_2^1 b_1 h_1^1) = 0 \tag{A9}$$

Substitution of x_1 from Equation A8 into Equations A6, A1a and A5 yields the following expressions:

$$c_{x2} = \frac{1}{a_2^1 b_1 h_1^1}\sum_{j=1}^{4}(m_j^3 + p m_j^2 - f m_j - g) N_j e^{m_j t} \tag{A10}$$

$$c_{y1} = \frac{1}{b_1}\sum_{j=1}^{4}(m_j + a_1) N_j e^{m_j t} \tag{A11}$$

$$c_{y2} = \frac{1}{b_1 h_1^1}\sum_{j=1}^{4}(m_j^2 + q m_j - r) N_j e^{m_j t} \tag{A12}$$